

# Phase Clusters in Large Populations of Chemical Oscillators\*\*

Annette F. Taylor, Mark R. Tinsley, Fang Wang, and Kenneth Showalter\*

Bacteria and other unicellular organisms communicate by exchange of chemical signaling species through the extracellular solution. In a phenomenon known as quorum sensing, synchronized activity is triggered when the population density or group size reaches a threshold value.<sup>[1]</sup> Many oscillatory chemical processes in cells, for example, glycolysis, become synchronized across a population by this type of coupling mechanism.<sup>[2]</sup> The dynamical mechanism of quorum sensing has been studied in biological and nonbiological systems,<sup>[2,3]</sup> in which a sudden “switching” transition from one dynamical state to another has been found; for example, individual yeast cells switch from steady-state to oscillatory behavior on reaching a threshold cell density. Another mechanism for synchronizing dynamical systems is Kuramoto synchronization,<sup>[4]</sup> in which unsynchronized oscillators gradually become synchronized at coupling strengths above a threshold value.<sup>[5]</sup> Many biological and nonbiological systems, from fireflies<sup>[6]</sup> to electrochemical oscillators,<sup>[7]</sup> have been found to synchronize by this mechanism. Recent studies have found both quorum sensing and Kuramoto synchronization in the same system for different regimes of coupling strength and number density,<sup>[3,8]</sup> and suggest that many types of systems, including coupled unicellular organisms, may be capable of both types of synchronization transitions.

The classical Kuramoto synchronization transition occurs smoothly above the critical coupling strength, and the frequency and phase of the oscillators become increasingly aligned with increasing coupling strength.<sup>[4]</sup> However, experimental studies on electrochemical oscillators<sup>[9,10]</sup> and photo-sensitive chemical oscillators<sup>[11]</sup> have found more complex oscillatory behavior in the transition. Rather than smoothly synchronizing, clusters of oscillators form that are frequency- and phase-synchronized but are out of phase with other clusters of oscillators. These groups of synchronized oscillators are known as phase clusters.<sup>[12]</sup>

Here we report on spontaneous formation of phase clusters in large populations of chemical oscillators (ca.  $10^5$

catalytic particles) coupled by exchange of chemical intermediates via the external solution. Each group has the same frequency but shows a phase shift with respect to the other groups, which gives rise to a global signal that is more complex than that of the individual oscillators. We experimentally examine the formation of clusters and their stability as a function of the number density of the oscillators. The behavior is compared with simulations based on a realistic computational model.

We study catalytic microparticles immersed in catalyst-free Belousov–Zhabotinsky (BZ) solutions<sup>[13]</sup> (see Experimental Section for details). The average concentration of chemical species in the surrounding solution is monitored electrochemically, and the oxidation state of the individual particles is obtained from images of the particle suspension: each particle changes color from orange to green and back again as the catalyst is oxidized and reduced during the oscillatory reaction cycle.<sup>[14]</sup> The population is heterogeneous with a distribution of oscillatory periods, as the period of a particle depends on its size and catalyst loading.<sup>[15]</sup>

Previously, we showed that the particles synchronize their rhythms when a well-stirred suspension is above a critical particle density.<sup>[3]</sup> The catalytic particles provide two critical species to the surrounding solution, the inhibitor  $\text{Br}^-$  and the activator (or autocatalyst)  $\text{HBrO}_2$ , which act as synchronizing species. The particle density (defined as mass of particles per milliliter of catalyst-free solution) must be above a threshold for synchronization to occur. The catalyst used in the current study is  $[\text{Ru}(\text{bpy})_3]^{2+}$  ( $\text{bpy} = 2,2'$ -bipyridine) rather than the ferroin catalyst used previously,<sup>[3]</sup> for which a smooth Kuramoto synchronization transition was observed.

The global signal for the surrounding solution is more complex for some conditions in the system containing catalyst particles loaded with  $[\text{Ru}(\text{bpy})_3]^{2+}$ . For low particle densities, a period-2 signal (two oscillations per period) is observed in the electrode potential (Figure 1a I). At higher particle densities, the signal is initially period-1 but then splits after several oscillations into two components of different amplitude (Figure 1a II), with global signal frequency doubling. With a further increase in number density, more period-1 oscillations occur before the signal splits into two components (Figure 1a III). Eventually, for sufficiently high particle density, only the period-1 signal is observed.

There are two possible interpretations of the electrochemical signal. One is that each of the individual oscillators develops the complex waveform, and the population oscillates in synchrony. The other is that the oscillators maintain their original waveform, and the global signal corresponds to the spontaneous formation of two groups of synchronized oscillators, separated by a constant phase difference. An analysis of the images accompanying the transition provides strong evidence for the latter.

[\*] Dr. M. R. Tinsley, F. Wang, Prof. K. Showalter  
C. Eugene Bennett Department of Chemistry  
West Virginia University  
Morgantown, WV 26506-6045 (USA)  
Fax: (+1) 304-293-4904  
E-mail: kshowalt@wvu.edu  
Homepage: <http://heracles.chem.wvu.edu>

Dr. A. F. Taylor  
Department of Chemistry, University of Leeds  
Leeds LS29JT (UK)

[\*\*] This work was supported by the National Science Foundation grant CHE-0809058 (K.S.) and the UK Engineering and Physical Sciences Research Council grant GR/T11036/01 (A.F.T.).

Supporting information for this article is available on the WWW under <http://dx.doi.org/10.1002/anie.201008248>.

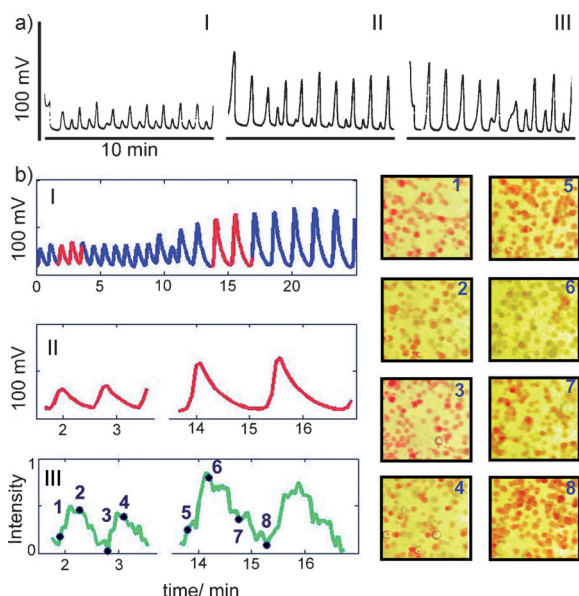


**Figure 1.** Formation of phase clusters in populations of catalytic micro-particles suspended in well-stirred, catalyst-free solutions with  $[\text{CH}_2(\text{COOH})_2] = 0.13 \text{ M}$ ,  $[\text{Br}^-] = 0.07 \text{ M}$ ,  $[\text{BrO}_3^-] = 0.45 \text{ M}$ ,  $[\text{H}_2\text{SO}_4] = 0.67 \text{ M}$ . a) Signal of Pt electrode showing complex behavior for increasing particle densities: I)  $0.03 \text{ g mL}^{-1}$ , II)  $0.032 \text{ g mL}^{-1}$ , III)  $0.04 \text{ g mL}^{-1}$ . b) Experiment with density of  $0.026 \text{ g mL}^{-1}$ . I) and II) Pt electrode trace, III) scaled intensity obtained from images of the particles, shown to the right (field of view ca.  $2 \times 2 \text{ mm}$ ), where an intensity of unity corresponds to all oxidized (green) particles.

Figure 1bI shows an electrochemical time series of an experiment in which the frequency of the global signal for the first 10 min is twice the frequency in the next 10 min. Two oscillations in each case are shown in Figure 1bII, and Figure 1bIII shows these oscillations reconstructed from an analysis of simultaneously captured images. Each image was analyzed to determine the fraction of oscillators in the oxidized state, with a scaled intensity of unity corresponding to all oxidized particles. The oscillation maximum in the first case corresponds to approximately half of the oscillators being in the oxidized state, while in the second case the oscillation maximum corresponds to almost all of the oscillators being in the oxidized state. A sampling of the images used to reconstruct the oscillations in Figure 1bIII is shown to the right, where the time at which each image was captured is shown in the time series.

Simulations of the catalyst–particle system provide insights into the formation of phase clusters. The model (see Supporting Information for details) consists of rate equations for each particle of the form [Eq. (1)]

$$\frac{dX_i}{dt} = f(X_i, Y_i, Z_i) - k_{\text{ex}}(X_i - X_s) \quad (1)$$

where  $X = \text{HBrO}_2$ ,  $Y = \text{Br}^-$ , and  $Z = \text{Ru}^{\text{III}}$ ,  $f(X_i, Y_i, Z_i)$  represents the reaction terms, and  $k_{\text{ex}}(X_i - X_s)$  the exchange of  $X$  or  $Y$  between the particle and the surrounding solution with rate constant  $k_{\text{ex}}$ . We assume species are homogeneously distributed in the surrounding solution with rate equations of the form [Eq. (2)]

$$\frac{dX_s}{dt} = g(X_s, Y_s) - \frac{\bar{V}}{V_s} \sum_{i=1}^N k_{\text{ex}}(X_s - X_i) \quad (2)$$

where  $g(X_s, Y_s)$  represents reaction terms for the surrounding solution and  $\bar{V}/V_s$  is the dilution factor (ratio of particle reaction volume to total volume of solution). For no exchange ( $k_{\text{ex}} = 0$ ), there is a distribution of periods of the chemical oscillators, which is determined by the catalyst concentration  $C$  on each particle. The BZ reaction exhibits relaxation oscillations and is unresponsive to perturbations immediately following the maximum amplitude. The system becomes responsive later in the cycle, however, with pulses of  $\text{Br}^-$  inducing phase delays and pulses of  $\text{HBrO}_2$  inducing (primarily) phase advances of the next oscillation.

As shown in Figure 2a, the model qualitatively reproduces the experimental behavior shown in Figure 1a, with the initial single peaks splitting to form smaller peaks every other oscillation. With increasing number density, the amplitude of bromide in the surrounding solution increases, and it takes longer for the peaks to split.

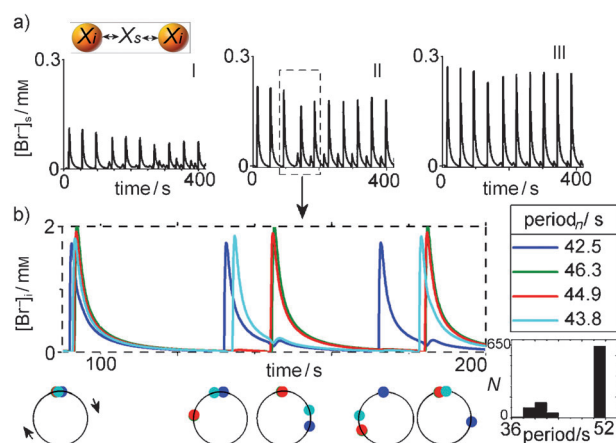


**Figure 2.** Formation of clusters in simulations with reaction on particles ( $C_{\text{catalyst}} = 3.3 \times 10^{-2} \text{ M}$ ) and transfer of species to the surrounding solution. a) Bromide concentration in the surrounding solution with increasing number density  $n = N/V_s$ , where  $N$  is the total number of oscillators ( $N = 1000$ ) and  $V_s$  the volume of the surrounding solution (variable) to give I)  $n = 9.5 \times 10^3 \text{ cm}^{-3}$ ; II)  $n = 1.9 \times 10^4 \text{ cm}^{-3}$ ; and III)  $n = 2.4 \times 10^4 \text{ cm}^{-3}$ . b) Bromide concentration on four individual oscillators for trace shown in a II); their phase representation ( $\cos \theta$  vs.  $\sin \theta$ ); the natural periods of the four oscillators (no transfer); and histogram of the periods of the whole population in the time interval 90–150 s.

In Figure 2b, cluster formation is analyzed by examining four of the individual oscillators in Figure 2aII. The concentration of bromide for each oscillator is plotted as a function of time and the corresponding phase plots are constructed: oscillators move clockwise around the cycle with constant velocity. The oscillators are initially in phase at  $t = 98 \text{ s}$ . Those oscillators with a shorter natural period are at the front of the group and “fire” first (the blue traces at  $t = 135 \text{ s}$ ). This results in an increase of bromide concentration in the surrounding solution, which gives rise to an increase in bromide concentration on the other oscillators. This pulse in bromide causes a

phase delay of the remaining oscillators, which fire later and form a second group. The distribution of periods during this initial split is shown in the histogram to the right, with a small group having periods around 40 s and the rest phase-delayed with a period of 50 s. The light blue oscillator falls back to join the second group by the next cycle, and the system of 1000 oscillators eventually relaxes to form two stable groups, whereby the ratio of occupation of the smaller group to the larger group is 35:65.

The particular phase cluster state exhibited does not depend on the initial conditions (i.e., the initial phase distribution), in contrast to numerical studies on phase oscillators<sup>[16]</sup> and experiments with locally coupled BZ oscillators.<sup>[17]</sup> Thus, for a particular set of parameters, either a stable group configuration is observed (no multistability), or the groups are unstable, containing a fraction of “switchers”, that is, oscillators that do not settle in a particular group, but jump between groups. In experiments, the amplitude of the electrochemical signal either is stable in time (Figure 3aI) or changes with time (Figure 3aII). The latter can be attributed to the appearance of switchers. Figure 3b shows two sets of

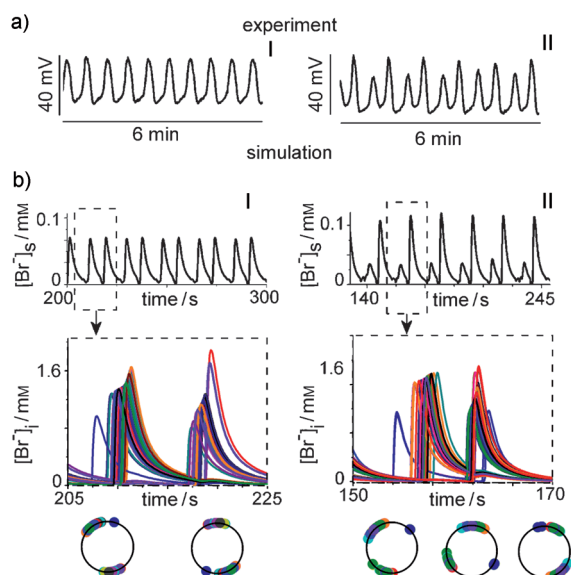


**Figure 3.** Switching oscillators. a) Electrode potential versus time traces ( $n = 0.02 \text{ g mL}^{-1}$ ) of two phase clusters showing I) stable signal amplitude in time and II) changing signal amplitude in time. b) Simulated results ( $N = 1000$ ) showing I) stable  $[Br^-]_s$  amplitude in time and II) changing  $[Br^-]_s$  amplitude in time. Lower plots show the bromide concentration in a sample of 100 individual oscillators and their phase representation. In II), the changing amplitude corresponds to the presence of switching oscillators: the blue oscillator at the front of the group jumps to join the group ahead.

simulations with the same parameters except for a slightly different set of natural frequencies. In Figure 3bI, the signal is stable in time and there is a stable configuration of oscillators in two groups. In Figure 3bII, the amplitude of the signal varies with time, the configuration of oscillators in the two groups is unstable, and oscillators jump between groups. Jumps arise either through the phase-delay effect from a pulse

in  $Br^-$ , as described in Figure 2b, or through a phase advance due to a pulse in  $HBrO_2$ .

Modeling simulations offer insights into the roles played by  $Br^-$  and  $HBrO_2$  in cluster formation. Figure 4a shows the number of clusters as a function of the number density,

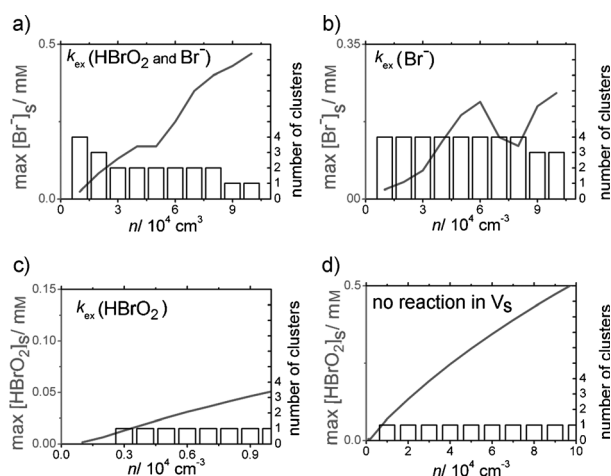


**Figure 4.** Behavior as a function of number density. Simulated results showing number of clusters and the maximum concentration of  $Br^-$  or  $HBrO_2$  in the surrounding solution as a function of number density with a) exchange of both  $HBrO_2$  and  $Br^-$  with the surrounding solution, b) exchange of  $Br^-$  only, c) exchange of  $HBrO_2$  only, and d) no reaction in the surrounding solution. Note that the maximum concentration depends on the relative oscillator populations of the clusters and therefore does not increase smoothly with  $n$  when clusters form.

whereby the number of clusters decreases with increasing number density and only one group with simple oscillations is observed for high number density. Up to four clusters are observed in simulations; however, one and two clusters are observed over a wide range of number densities, and it is therefore not surprising that these are mainly observed in the experiments. With exchange of only  $Br^-$  ( $k_{ex} = 0$  for  $HBrO_2$ ), the number of clusters decreases more gradually with increasing number density (Figure 4b), and two clusters continue to be observed even for very high  $n$ . Figure 4c shows the behavior with exchange of only  $HBrO_2$  ( $k_{ex} = 0$  for  $Br^-$ ), and only one cluster is observed for all values of  $n$ . Only one cluster is also observed when no reaction occurs between  $HBrO_2$  and  $Br^-$  in the surrounding solution, as shown in Figure 4d. We conclude that formation of the simple one-group state can be attributed to the synchronizing effect of  $HBrO_2$ , the amplitude of which increases in the surrounding solution with increasing number density. The appearance of cluster states, as shown in Figure 4a, arises from the weaker coupling resulting from  $Br^-$  in the surrounding solution. When only  $HBrO_2$  is exchanged between the surrounding solution and the catalytic particles (Figure 4c) or no consumption of  $HBrO_2$  occurs (Figure 4d), no cluster formation is observed. We note that while both  $HBrO_2$  and  $Br^-$  act as synchronizing species, a perturbation in  $HBrO_2$  results in a phase advance, and a perturbation in  $Br^-$  in a phase delay (see Supporting Information).

Formation of clusters in globally coupled oscillators has been experimentally observed in electrochemical oscillators<sup>[7,10]</sup> and light-sensitive BZ particles.<sup>[11]</sup> Here we have demonstrated how a large population of chemical oscillators, coupled by the exchange of chemical intermediates via the external solution, can form groups of synchronized oscillators separated by a phase difference. This form of chemical communication is widespread in nature, for example, intercellular signaling in cell suspensions via the extracellular solution. The ability of chemical oscillators to construct complex global signals from simple periodic oscillations may play a role in the functioning of natural systems, for example, in cellular differentiation.<sup>[18]</sup> Hence, the same global signal that connects and synchronizes a heterogeneous population of oscillators can nevertheless provide different chemical environments for individual groups within the population.

## Experimental Section

Experiments were carried out with cation-exchange particles (Dowex 50W) of diameter 100–200  $\mu\text{m}$  that were loaded with the BZ catalyst  $[\text{Ru}(\text{bpy})_3]^{2+}$ . A known mass of particles was added to a volume of catalyst-free BZ solution consisting of malonic acid,  $\text{NaBrO}_3$ ,  $\text{NaBr}$ , and  $\text{H}_2\text{SO}_4$ . In the absence of stirring, particles display a range of frequencies, which can be measured from the change in particle intensity with time (Figure 5a). Particles are stirred with a magnetic or overhead stirrer, and images obtained by using a CCD camera

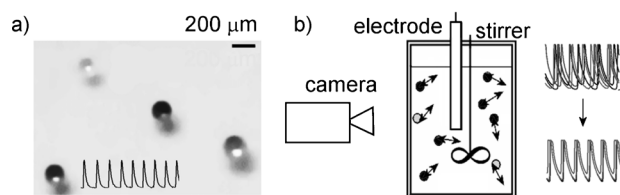


**Figure 5.** a) Experimental image of catalytic microparticles in catalyst free solution with periodic change in particle intensity with time (superimposed). b) Sketch of setup for stirred experiments, illustrating the transition from a distribution of particle frequencies to synchronized oscillations.

(Figure 5b). The concentration of bromine-containing species in the surrounding solution was followed by using a combination electrode.

Received: December 30, 2010

Published online: May 3, 2011

**Keywords:** dynamical quorum sensing · electrochemistry · oscillating reactions · ruthenium · synchronization

- [1] M. B. Miller, B. L. Bassler, *Annu. Rev. Microbiol.* **2001**, 55, 165–199.
- [2] S. De Monte, F. d'Ovidio, S. Danø, P. G. Sørensen, *Proc. Natl. Acad. Sci. USA* **2007**, 104, 18377–18381.
- [3] A. F. Taylor, M. R. Tinsley, F. Wang, Z. Huang, K. Showalter, *Science* **2009**, 323, 614–617.
- [4] Y. Kuramoto, *Chemical Oscillations, Waves and Turbulence*, Springer, Berlin, **1984**.
- [5] A. S. Pikovsky, M. Rosenblum, J. Kurths, *Synchronization: A Universal Concept In Nonlinear Sciences*, Cambridge University Press, Cambridge, **2001**.
- [6] S. H. Strogatz, *Physica D* **2000**, 143, 1–20.
- [7] I. Z. Kiss, Y. M. Zhai, J. L. Hudson, *Science* **2002**, 296, 1676–1678.
- [8] J. Zamora-Munt, C. Masoller, J. Garcia-Ojalvo, R. Roy, *Phys. Rev. Lett.* **2010**, 105, 264101.
- [9] I. Z. Kiss, Y. M. Zhai, J. L. Hudson, *Prog. Theor. Phys. Suppl.* **2006**, 161, 99–106.
- [10] I. Z. Kiss, C. G. Rusin, H. Kori and J. L. Hudson, *Science* **2007**, 316, 1886–1889.
- [11] A. F. Taylor, P. Kapetanopoulos, B. J. Whitaker, R. Toth, L. Bull, M. R. Tinsley, *Phys. Rev. Lett.* **2008**, 100, 214101.
- [12] D. Golomb, D. Hansel, B. Shraiman, H. Sompolsky, *Phys. Rev. A* **1992**, 45, 3516–3530.
- [13] J. Maselko, J. S. Reckley, K. Showalter, *J. Phys. Chem.* **1989**, 93, 2774–2780.
- [14] R. Toth, A. F. Taylor, M. R. Tinsley, *J. Phys. Chem. B* **2006**, 110, 10170–10176.
- [15] K. Yoshikawa, R. Aihara, K. Agladze, *J. Phys. Chem. A* **1998**, 102, 7649–7652.
- [16] E. Ullner, A. Zaikin, E. I. Volkov, J. Garcia-Ojalvo, *Phys. Rev. Lett.* **2007**, 99, 148103.
- [17] M. Toiya, V. K. Vanag, I. R. Epstein, *Angew. Chem.* **2008**, 120, 7867–7869; *Angew. Chem. Int. Ed.* **2008**, 47, 7753–7755.
- [18] S. C. Manrubia, A. S. Mikhailov, D. H. Zannette, *Emergence of Dynamical Order: Synchronization Phenomena in Complex Systems*, World Scientific Publishing Company, Singapore, **2004**.